Tree Tensor Network Decomposition of Open Quantum Dynamics for Efficient Simulation of Next-Generation Quantum Systems

Xinxian Chen

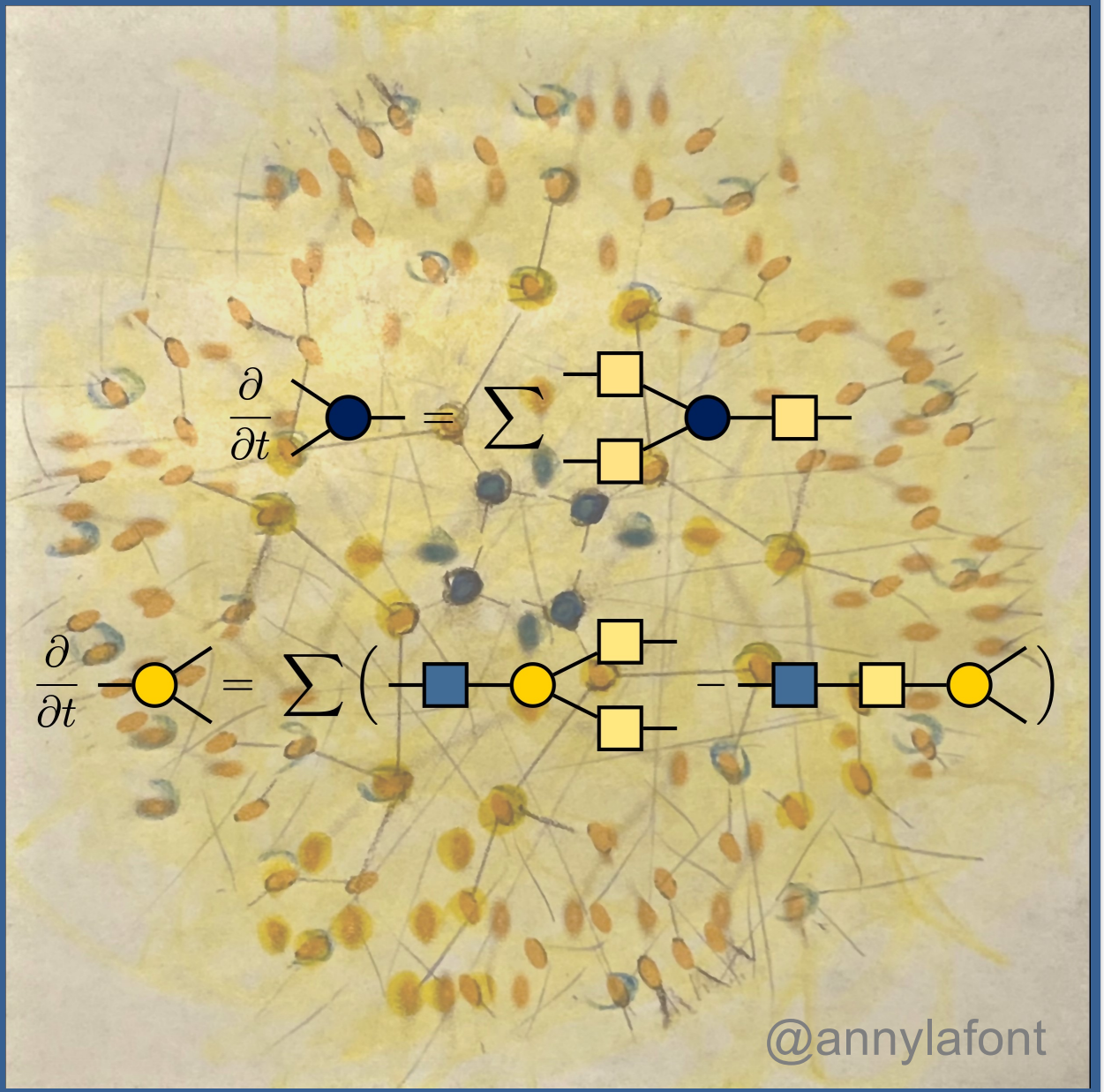

Ignacio Franco
University of Rochester

VISTA #102. February 11, 2026

Research in the Franco Group

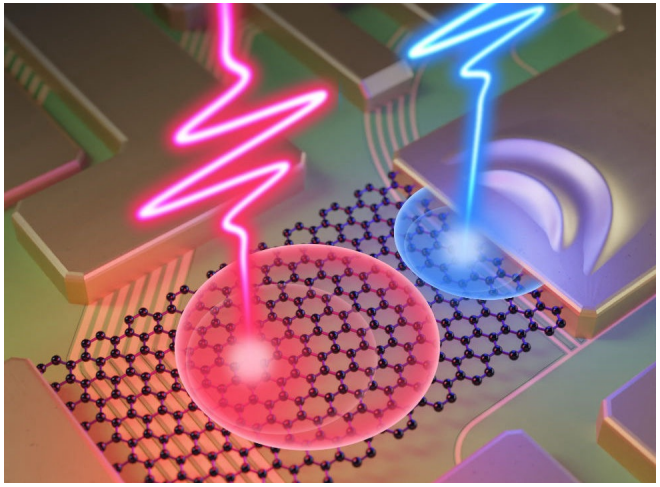

Quantum Control of Matter at the Level of Electrons

e.g. Nature **605**, 251 (2022)
PRL **135**, 186901 (2025)

Quantum Coherence in Matter

e.g. PNAS **120**, e2309987120 (2023)
J. Chem. Phys. **163** 104109 (2025)

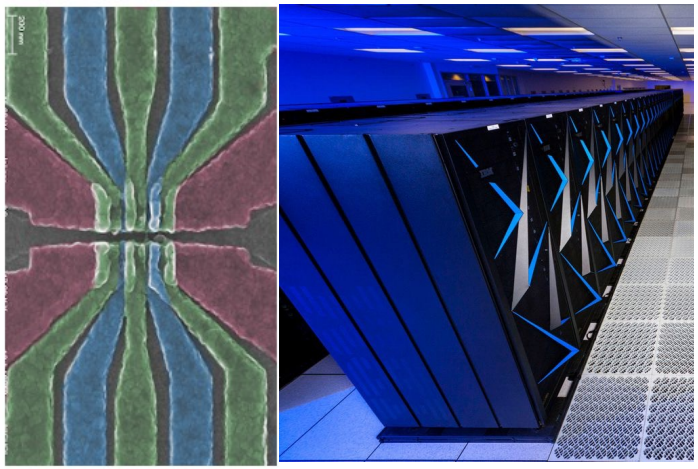

Quantum Simulation

e.g. PRX Quantum **3**, 040308 (2022)

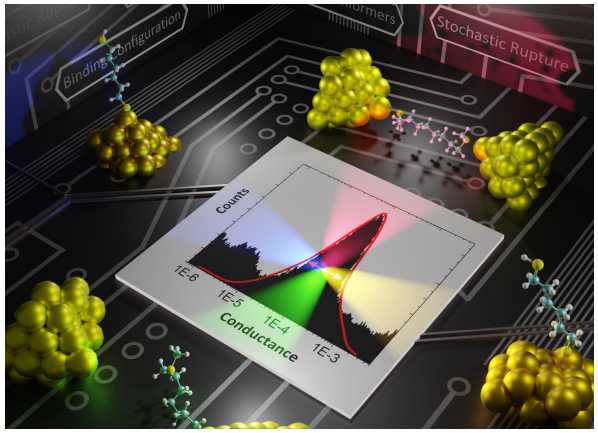

Quantum Transport

e.g. Nature Comm. **14**, 7646 (2023)
JACS **147**, 20310 (2025)

Open Quantum Dynamics

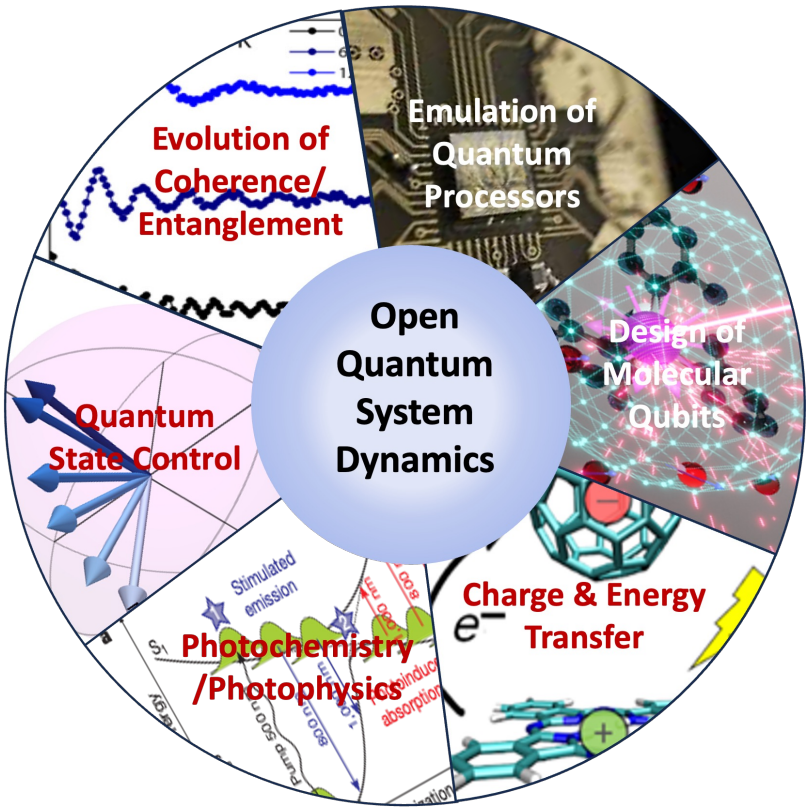

Chemical Principles of Quantum Decoherence

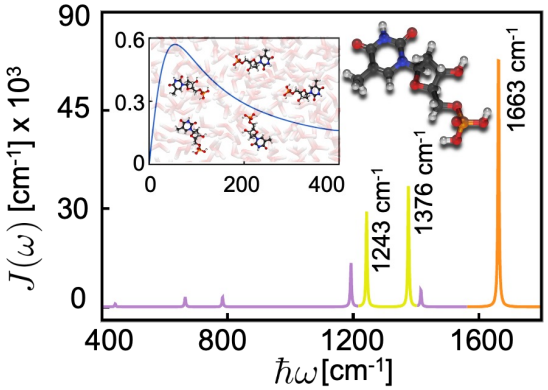

PNAS **120**, e2309987120 (2023)

Foundations of Decoherence

e.g. JCP **162**, 064106 (2025);
JPCL 13, 11503 (2022);
JCP **151**, 014109 (2019);
JCP, **148**, 134304 (2018);
JPCL **9**, 773 (2018)

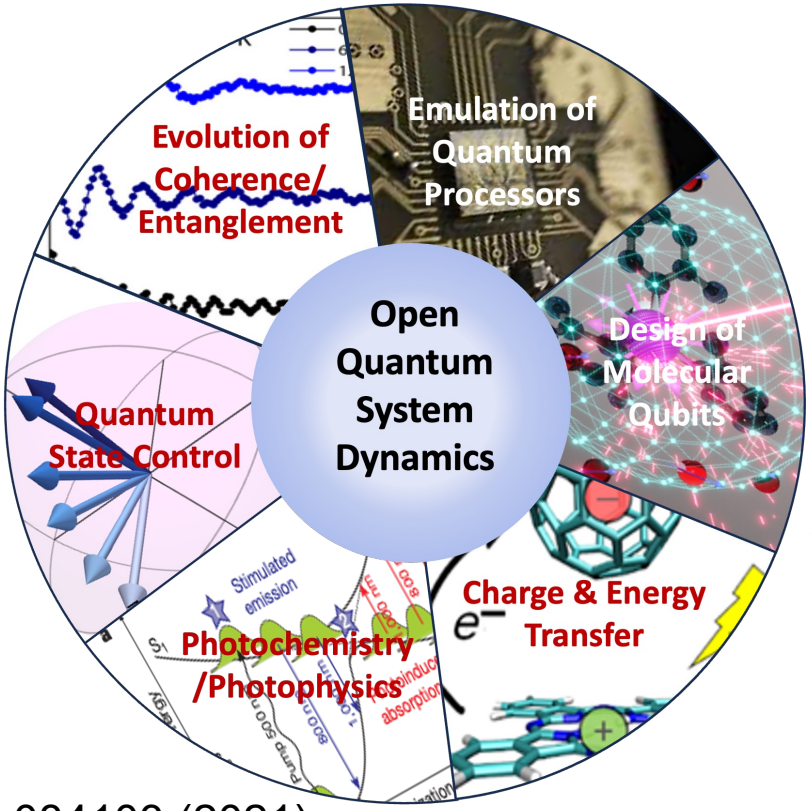

Quantum Simulation

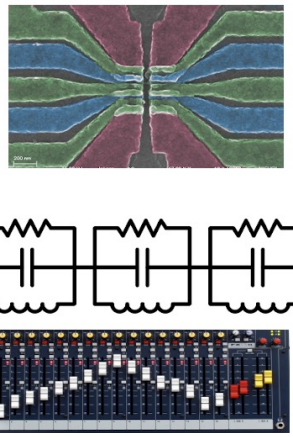

PRX Quantum **3**, 040308 (2022); JPC A **129**, 15, 3587 (2025)

Theory of Dissipation Pathways

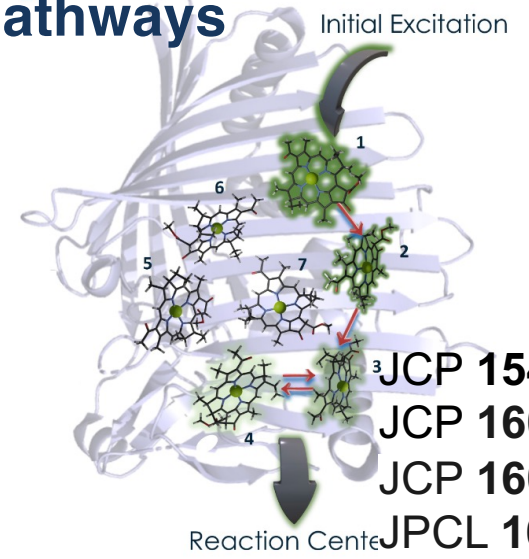

JCP **154**, 084103 (2021);
JCP **160**, 214111 (2024);
JCP **160**, 214112 (2024);
JPCL **16**, 13093 (2025);
JCP **164**, 034105 (2026)

Tensor Network Strategies

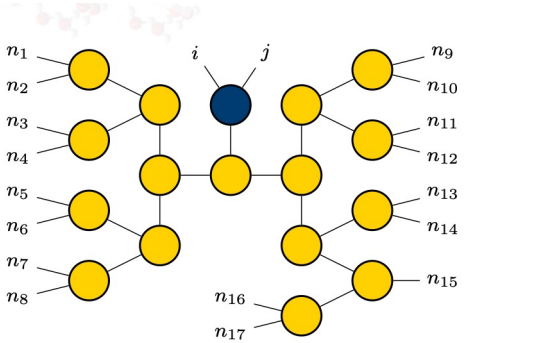

JCP **160**, 204116 (2024);
JCP **163**, 104109 (2025);
JCP **164**, 024112 (2026)

Methods in Open Quantum Dynamics

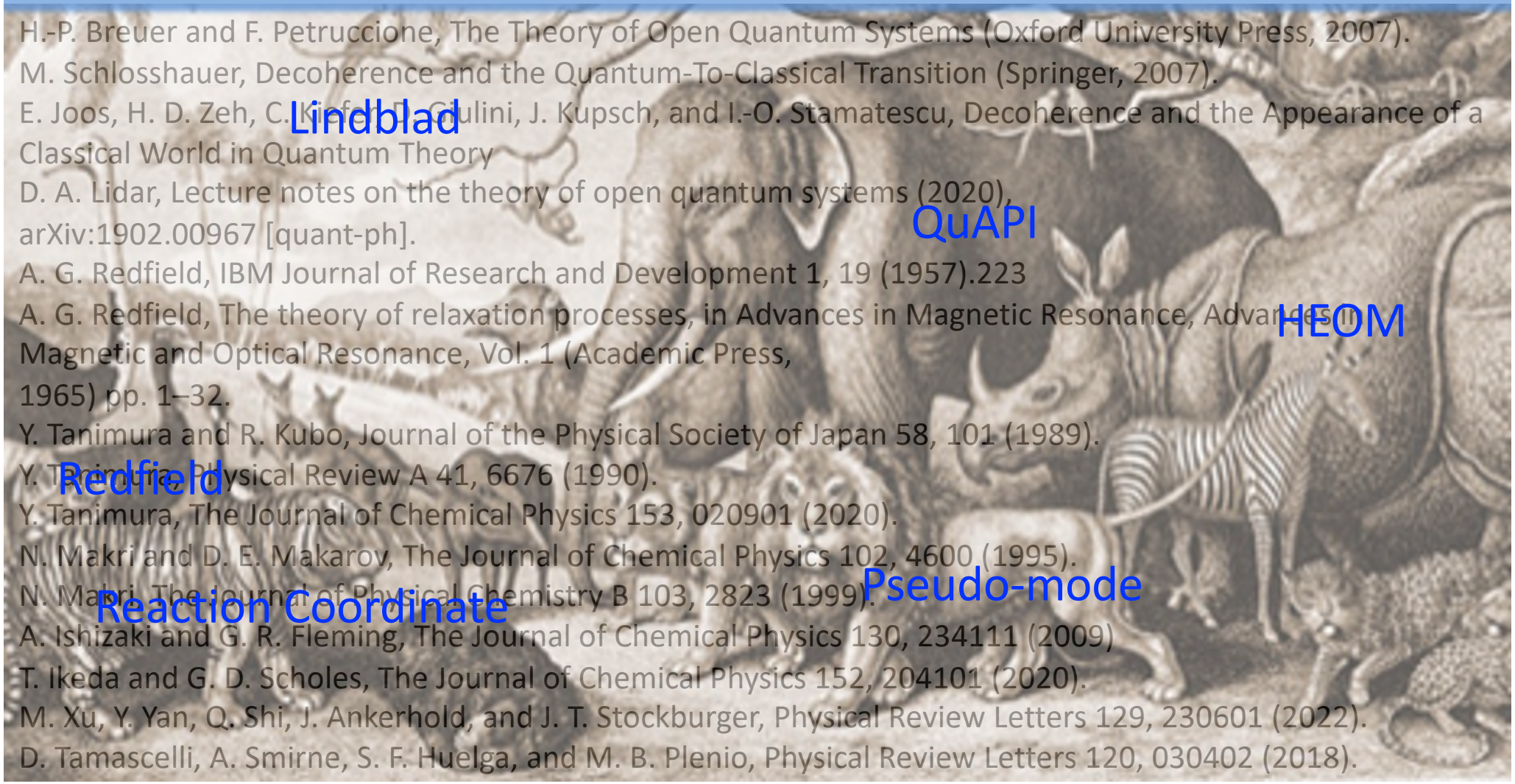

H.-P. Breuer and F. Petruccione, The Theory of Open Quantum Systems (Oxford University Press, 2007).
M. Schlosshauer, Decoherence and the Quantum-To-Classical Transition (Springer, 2007).
E. Joos, H. D. Zeh, C. Kiefer, D. Giulini, J. Kupsch, and I.-O. Stamatescu, Decoherence and the Appearance of a Classical World in Quantum Theory
D. A. Lidar, Lecture notes on the theory of open quantum systems (2020), arXiv:1902.00967 [quant-ph].
A. G. Redfield, IBM Journal of Research and Development 1, 19 (1957).223
A. G. Redfield, The theory of relaxation processes, in Advances in Magnetic Resonance, Advances in Magnetic and Optical Resonance, Vol. 1 (Academic Press, 1965) pp. 1–32.
Y. Tanimura and R. Kubo, Journal of the Physical Society of Japan 58, 101 (1989).
Y. Tanimura, Physical Review A 41, 6676 (1990).
Y. Tanimura, The Journal of Chemical Physics 153, 020901 (2020).
N. Makri and D. E. Makarov, The Journal of Chemical Physics 102, 4600 (1995).
N. Makri, The Journal of Physical Chemistry B 103, 2823 (1999).
A. Ishizaki and G. R. Fleming, The Journal of Chemical Physics 130, 234111 (2009)
T. Ikeda and G. D. Scholes, The Journal of Chemical Physics 152, 204101 (2020).
M. Xu, Y. Yan, Q. Shi, J. Ankerhold, and J. T. Stockburger, Physical Review Letters 129, 230601 (2022).
D. Tamascelli, A. Smirne, S. F. Huelga, and M. B. Plenio, Physical Review Letters 120, 030402 (2018).

Lindblad

QuAPI

HEOM

Redfield

Pseudo-mode

Reaction Coordinate

N. Lambert, S. Ahmed, M. Cirio, and F. Nori, Nature Communications 10, 3721 (2019).
G. Park, Z. Huang, Y. Zhu, C. Yang, G. K.-L. Chan, and L. Lin, Physical Review B 110, 195148 (2024).
Z. Huang, G. Park, G. K.-L. Chan, and L. Lin, arXiv:2506.10308
X. Zheng, J. Jin, S. Welack, M. Luo, and Y. Yan, The Journal of Chemical Physics 130, 164708 (2009).
J. Hu, R.-X. Xu, and Y. Yan, The Journal of Chemical Physics 133, 101106 (2010).
J. Hu, M. Luo, F. Jiang, R.-X. Xu, and Y. Yan, The Journal of Chemical Physics 134, 244106 (2011).

The Hierarchical Equation of Motion (HEOM)

- System agnostic
- Admits driven systems
- Numerically exact for harmonic environments
- Admits non-commuting system-bath interactions
- Goes beyond Lindblad/Redfield Markovian models

- Memory hungry
- Computational cost scales exponentially with size of system and complexity of the environment

Ishizaki and Tanimura, JCP 125 084501 (2006)
Tanaka and Tanimura, JCP **132** 214502 (2010)
Tanimura JCP **141** 044114 (2014)
Ikeda and Scholes, JCP, **152**, 204101 (2020)
Tanimura, JCP **153**, 020901 (2020)
Yan, Xu, Li, and Shi, JCP **154**, 194104 (2021)
Chen and Franco, JCP **160**, 204116 (2024)

Harmonic Environments

Useful model of the environment: Collection of harmonic oscillators

- Any environment can be mapped into an effective harmonic environment (to second order in perturbation theory)
- Dominant behavior in the thermodynamic limit
- The reason why the displaced harmonic oscillator model is so successful in spectroscopy

Hamiltonian

$$H = H_{\mathrm{S}} + H_{\mathrm{SB}} + H_{\mathrm{B}},$$

$$H_{\mathrm{B}} = \sum_{j=1}^{\infty} \omega_j a_j^{\dagger} a_j \qquad H_{\mathrm{SB}} = Q_{\mathrm{S}} \otimes X_{\mathrm{B}}$$

$$X_{\mathrm{B}} = \sum_{j=1}^{\infty} (g_j a_j^{\dagger} + g_j^{\star} a_j)$$

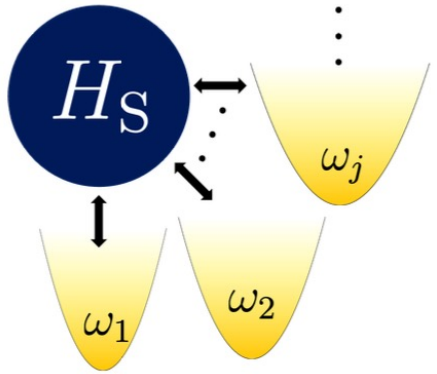

Feynman and Vernon. Ann. Phys. 24 118–173 (1963)
Caldeira and Leggett. Ann. Phys. 149 374–456 (1983)
Suárez and Silbey, J Chem. Phys. 95, 9115 (1991)
Makri J. Phys. Chem. B 103, 2823-2829 (1999)

Dynamical Map for Harmonic Environments

Hamiltonian $H = H_{\rm S} + H_{\rm SB} + H_{\rm B},$

$$H_{\rm B} = \sum_{j=1}^{\infty} \omega_j a_j^\dagger a_j \qquad H_{\rm SB} = Q_{\rm S} \otimes X_{\rm B} \qquad X_{\rm B} = \sum_{j=1}^{\infty} (g_j a_j^\dagger + g_j^\star a_j)$$

Initially separable state $\rho(0) = \rho_{\rm S}(0) \otimes \rho_{\rm B}^{\rm eq}$

Exact dynamical map in interaction picture

$$\tilde{\rho}_{\rm S}(t) = \mathcal{T}\tilde{\mathcal{F}}(t,0)\rho_{\rm S}(0) \equiv \mathcal{T}\exp\left(-\int_0^t dt_2 \tilde{Q}_{\rm S}^\times(t_2) \int_0^{t_2} dt_1 [C(t_2-t_1)\tilde{Q}_{\rm S}(t_1)]^\times\right)\rho_{\rm S}(0)$$

Notation $A^\times B = AB - BA^\dagger$

Correlation Function $C(t) = \langle X_{\rm B}(t) X_{\rm B}(0)\rangle_{\rm B}.$

Spectral Density $C(t) = \int_{-\infty}^{\infty} \mathcal{J}(\omega) f_{\rm BE}(\beta\omega) e^{-i\omega t} d\omega.$

$$J(\omega) = \textstyle\sum_j |g_j|^2 \delta(\omega - \omega_j) \quad (\omega > 0) \qquad f_{\rm BE}(\beta\omega) = (1 - e^{-\beta\omega})^{-1}$$

$$\mathcal{J}(\omega) = J(\omega) - J(-\omega)$$ odd extension

Ishizaki and Fleming, J. Chem. Phys. **130**, 234111 (2009)
Molinari, arXiv:1710.09248 (2017)
Isserlis, Biometrika **12**, 134 (1918)

Spectral Density: characterizes system-bath interaction

$J(\omega)$

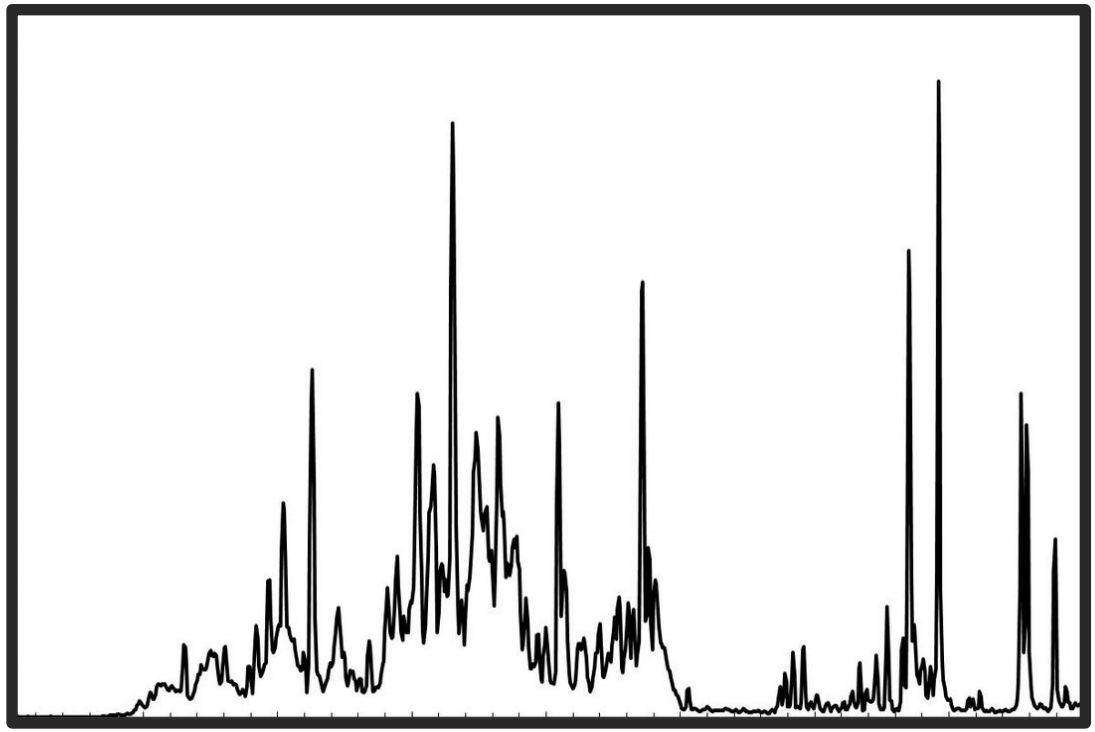

$\hbar\omega$

Summarizes frequencies of the bath and interaction strength with the system

The HEOM way

Spectral Density

$$C(t) = \int_{-\infty}^{\infty} \mathcal{J}(\omega) f_{\mathrm{BE}}(\beta\omega) e^{-i\omega t} d\omega.$$

Decomposition the BCF into complex exponentials or features

$$C(t) = \sum_{k=1}^{K} c_k e^{\gamma_k t} \qquad C^*(t) = \sum_{k=1}^{K} \bar{c}_k e^{\gamma_k t}.$$

- Solvent: Drude–Lorentz model

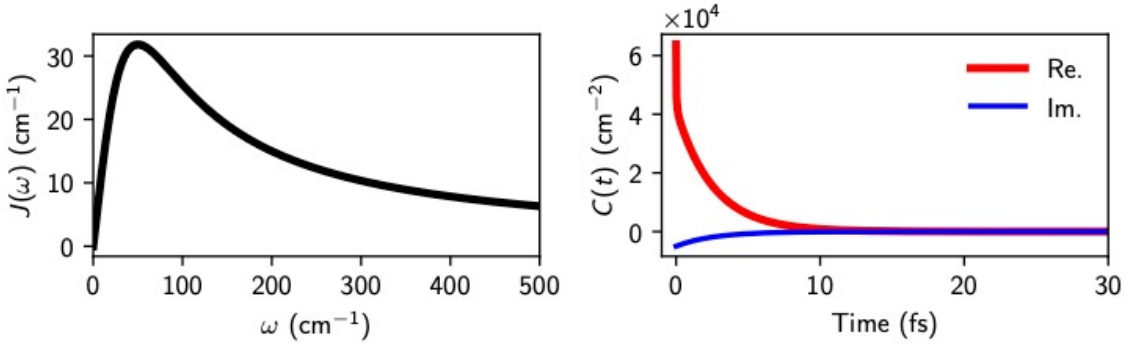

1 feature

- Intramolecular vibrations: Brownian oscillators

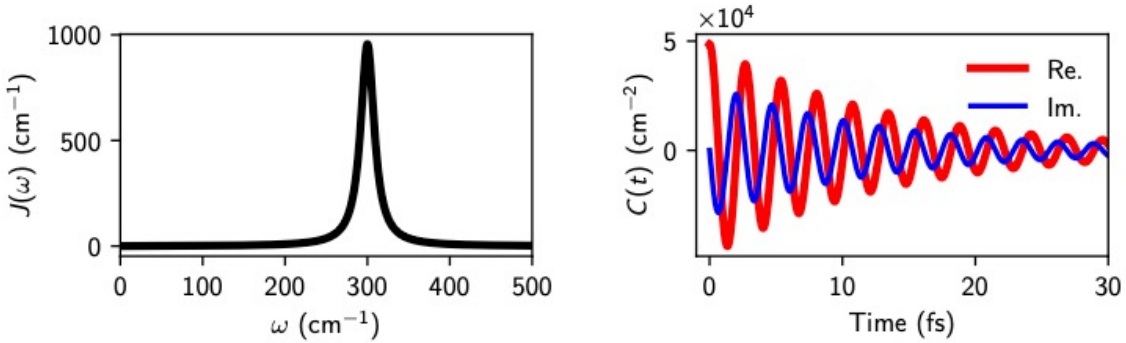

2 features

The HEOM way

Decomposition the BCF into complex exponentials or features is exact

$$C^*(t) = \sum_{k=1}^{K} \bar{c}_k e^{\gamma_k t}. \qquad C(t) = \sum_{k=1}^{K} c_k e^{\gamma_k t}$$

From residue theorem/Padé or Matsubara expansions

$$C(t) = -2\pi\mathrm{i} \sum_i \operatorname*{Res}_{z=\zeta_i} [\mathcal{J}(z)] f_{\mathrm{BE}}(\beta\zeta_i) e^{-\mathrm{i}\zeta_i t} - 2\pi\mathrm{i} \sum_j \operatorname*{Res}_{z=\xi_j} [f_{\mathrm{BE}}(z)] \mathcal{J}(\xi_j/\beta) e^{-\mathrm{i}(\xi_j/\beta)t},$$

Features from the spectral density

Features from low temperature corrections

Several available methods:

JCP 130, 164708 (2009); JCP 133, 101106 (2010); JCP 151, 024110 (2019)
JCP 152, 064107 (2020); PRL 129, 230601 (2022); JCP 160, 204105 (2024)

The HEOM way

Decomposition the BCF into complex exponentials or features is exact

$$C^*(t) = \sum_{k=1}^{K} \bar{c}_k e^{\gamma_k t}. \qquad C(t) = \sum_{k=1}^{K} c_k e^{\gamma_k t}$$

From residue theorem/Padé or Matsubara expansions

$$C(t) = -2\pi\mathrm{i} \sum_i \operatorname*{Res}_{z=\zeta_i} [\mathcal{J}(z)] f_{\mathrm{BE}}(\beta\zeta_i) e^{-\mathrm{i}\zeta_i t} - 2\pi\mathrm{i} \sum_j \operatorname*{Res}_{z=\xi_j} [f_{\mathrm{BE}}(z)] \mathcal{J}(\xi_j/\beta) e^{-\mathrm{i}(\xi_j/\beta)t},$$

Use this decomposition to decompose the dynamical map

Introduce auxiliary density matrix (ADM) to keep bath information

$$\rho_{\vec{n}} = \rho_{n_1,\ldots,n_K} \qquad n_k = 0, 1, 2, \ldots, N$$

The HEOM way

$$\frac{\partial}{\partial t}\rho_{\vec{n}}(t) = -\mathrm{i}H_{\mathrm{S}}^{\times} + \sum_{k}\left(n_k\gamma_k\rho_{\vec{n}}(t) - \mathrm{i}n_k\left(c_kQ_{\mathrm{S}}^{>} - \bar{c}_kQ_{\mathrm{S}}^{<}\right)\rho_{\vec{n}-\hat{1}_k}(t) - \mathrm{i}Q_{\mathrm{S}}^{\times}\rho_{\vec{n}+\hat{1}_k}(t)\right)$$

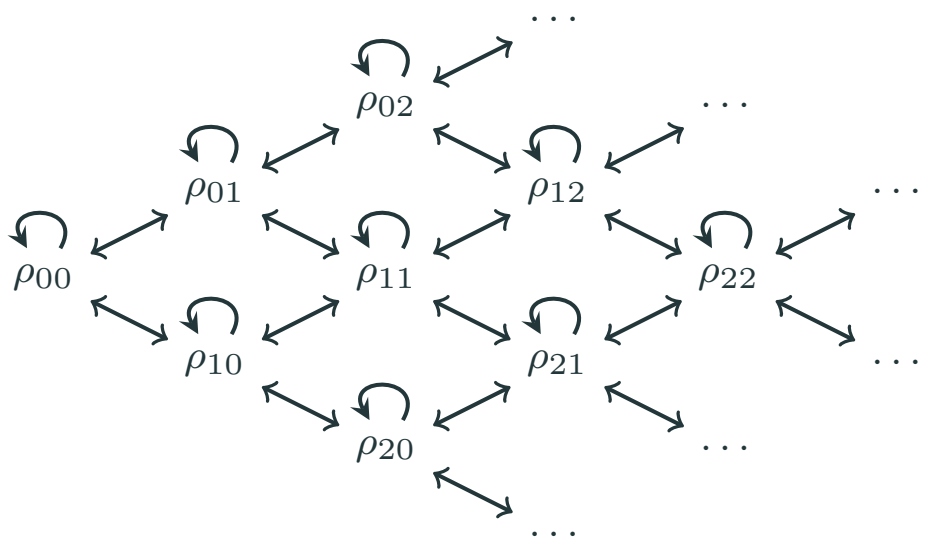

Curse of dimensionality: The hierarchy generate an infinite K-dimensional grid

Tanimura and Kubo. J. Phys. Soc. Jpn. **58**, 101–114 (1989)
Tanimura. J. Chem. Phys. **153**, 020901 (2020)

Bexcitonic generalization of the HEOM

X. Chen and I. Franco, J. Chem. Phys. **160**, 204116 (2024)

Decomposition of the BCF into *K* features

$$C(t) = \sum_{k=1}^{K} c_k \psi_k(t) \qquad C^\star(t) = \sum_{k=1}^{K} \bar{c}_k \psi_k(t) \qquad \frac{\mathrm{d}}{\mathrm{d}t}\psi_k(t) = \sum_{k'=1}^{K} \gamma_{kk'}\psi_{k'}(t)$$

$$\psi_k(0) = 1$$

$$\tilde{\rho}_{\mathrm{S}}(t) = \mathcal{T}\tilde{\mathcal{F}}(t,0)\rho_{\mathrm{S}}(0) \equiv \mathcal{T}\exp\left(-\int_0^t dt_2 \tilde{Q}_{\mathrm{S}}^{\times}(t_2)\int_0^{t_2} dt_1 [C(t_2-t_1)\tilde{Q}_{\mathrm{S}}(t_1)]^{\times}\right)\rho_{\mathrm{S}}(0)$$

Define Auxiliary Density Matrices (ADMs)

$$\tilde{\varrho}_{\vec{n}}(t) \equiv \mathcal{T}\left(\prod_{k=1}^{K}\frac{\tilde{f}_k^{\,n_k}(t,0)}{Z_k(n_k)\sqrt{n_k!}}\right)\tilde{\mathcal{F}}(t,0)\rho_{\mathrm{S}}(0) \qquad \vec{n} \equiv (n_1,\ \ldots,\ n_K)$$

$$\tilde{f}_k(t,0) = c_k\tilde{\theta}_k^{>}(t,0) - \bar{c}_k\tilde{\theta}_k^{<}(t,0) \qquad \tilde{\theta}_k(s,0) = \int_0^s \tilde{Q}_{\mathrm{S}}(u)\psi_k(s-u)\mathrm{d}u$$

Z_k is a non-zero c-number: metric

Bexcitonic generalization of HEOM

X. Chen and I. Franco, J. Chem. Phys. **160**, 204116 (2024)

Put all the ADMs in a vector
Extended Density Operator

$$|\Omega(t)\rangle \equiv \sum_{\vec{n}} \varrho_{\vec{n}}(t)|\vec{n}\rangle$$

$$|\vec{n}\rangle \equiv |n_1\rangle \otimes \cdots \otimes |n_K\rangle$$

$$\hat{\alpha}_k^\dagger|n_k\rangle = \sqrt{n_k+1}|n_k+1\rangle \qquad \hat{\alpha}_k|n_k\rangle = \sqrt{n_k}|n_k-1\rangle$$

$$\hat{n}_k = \hat{\alpha}_k^\dagger\hat{\alpha}_k$$

Bexciton raising/lowering operators

Equations of motion

$$\frac{\mathrm{d}}{\mathrm{d}t}|\Omega(t)\rangle = \left(-\mathrm{i}H_{\mathrm{S}}^{\times}(t) + \sum_{k=1}^{K}\mathcal{D}_k\right)|\Omega(t)\rangle \qquad |\Omega(0)\rangle = \rho_{\mathrm{S}}(0)|0\rangle \otimes \cdots \otimes |0\rangle$$

$$\mathcal{D}_k = \gamma_{kk}\hat{n}_k + \sum_{k'\neq k}\gamma_{kk'}\hat{z}_k^{-1}\hat{\alpha}_k^\dagger\hat{\alpha}_{k'}\hat{z}_{k'} + (c_k Q_{\mathrm{S}}^{>} - \bar{c}_k Q_{\mathrm{S}}^{<})\hat{z}_k^{-1}\hat{\alpha}_k^\dagger - Q_{\mathrm{S}}^{\times}\hat{\alpha}_k\hat{z}_k$$

$\hat{z}_k$ metric (commutes with n_k)

Varying BCF decomposition, metric, representation leads to various HEOM variants

Bexcitonic picture

X. Chen and I. Franco, J. Chem. Phys. **160**, 204116 (2024)

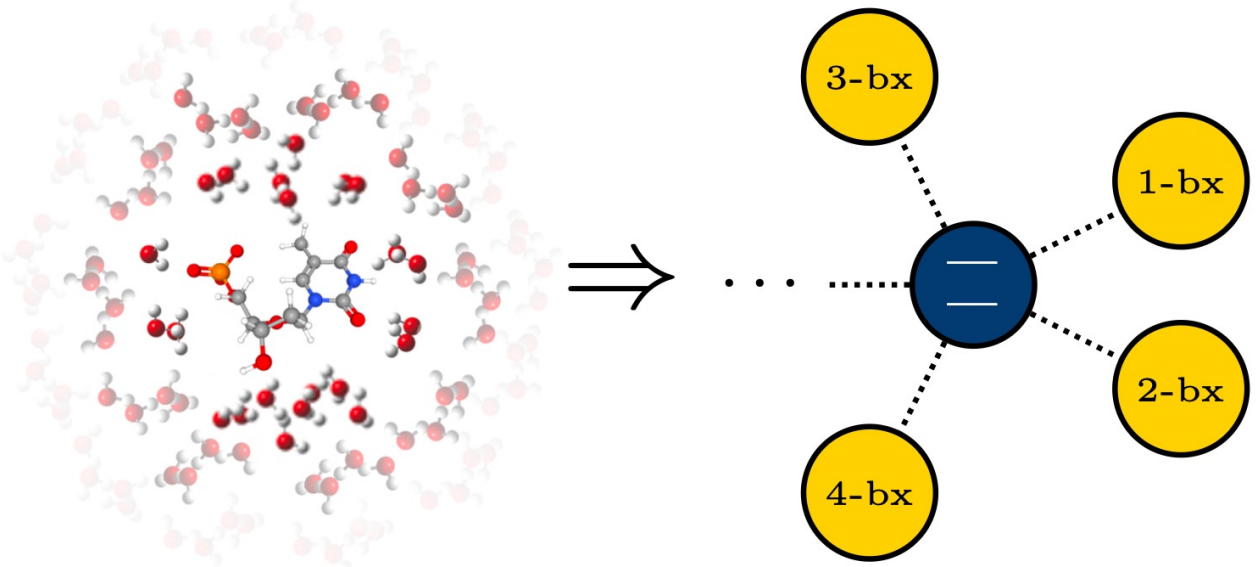

$$\frac{\mathrm{d}}{\mathrm{d}t}|\Omega(t)\rangle = \left(-\mathrm{i}H_{\mathrm{S}}^{\times}(t) + \sum_{k=1}^{K}\mathcal{D}_k\right)|\Omega(t)\rangle$$

$$\mathcal{D}_k = \gamma_{kk}\hat{n}_k + \sum_{k'\neq k}\gamma_{kk'}\hat{z}_k^{-1}\hat{\alpha}_k^{\dagger}\hat{\alpha}_{k'}\hat{z}_{k'} + (c_k Q_{\mathrm{S}}^{>} - \bar{c}_k Q_{\mathrm{S}}^{<})\hat{z}_k^{-1}\hat{\alpha}_k^{\dagger} - Q_{\mathrm{S}}^{\times}\hat{\alpha}_k\hat{z}_k$$

Open Quantum Dynamics = Dynamics of the System + Bexcitons
(fictitious bosonic quasiparticles)

Depth of HEOM *N* = Number of bexcitonic levels

Develop many HEOM variants

$$\frac{\mathrm{d}}{\mathrm{d}t}|\Omega(t)\rangle = \left(-\mathrm{i}H_{\mathrm{S}}^{\times}(t) + \sum_{k=1}^{K}\mathcal{D}_k\right)|\Omega(t)\rangle$$

$$\mathcal{D}_k = \gamma_{kk}\hat{n}_k + \sum_{k'\neq k}\gamma_{kk'}\hat{z}_k^{-1}\hat{\alpha}_k^{\dagger}\hat{\alpha}_{k'}\hat{z}_{k'} + (c_k Q_{\mathrm{S}}^{>} - \bar{c}_k Q_{\mathrm{S}}^{<})\hat{z}_k^{-1}\hat{\alpha}_k^{\dagger} - Q_{\mathrm{S}}^{\times}\hat{\alpha}_k\hat{z}_k$$

Flexibility:

- Varying BCF decomposition
- Representation: position, momentum, number, etc
- Metric

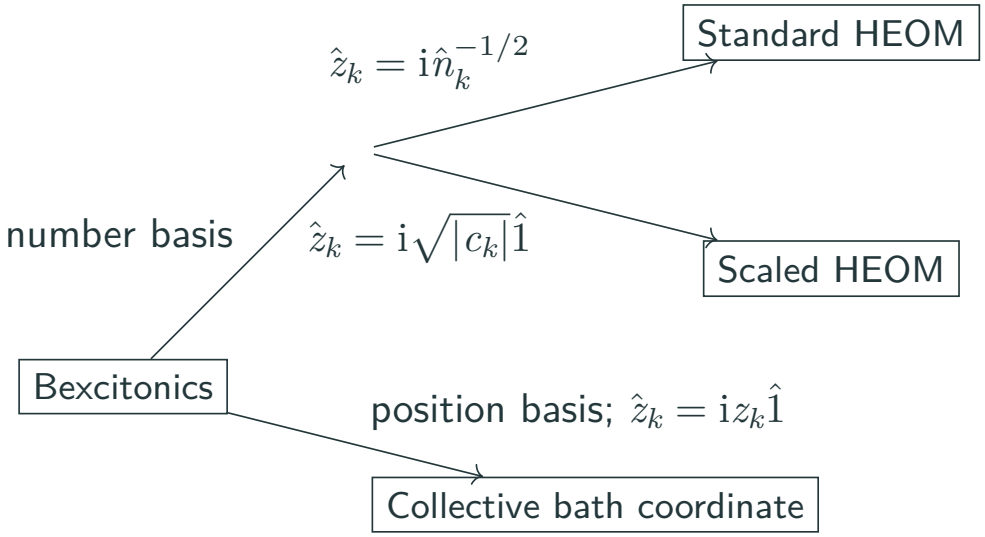

Q. Shi, et al., J. Chem. Phys. **130**, 84105 (2009)

T. Ikeda and A. Nakayama, J. Chem. Phys. **156**, 104104 (2022)

Numerical verification

$$H_{\mathrm{S}} = \frac{E}{2}\sigma_z + V\sigma_x \qquad Q_{\mathrm{S}} = \sigma_z \qquad |\psi\rangle = \frac{1}{\sqrt{2}}(|g\rangle + |e\rangle)$$

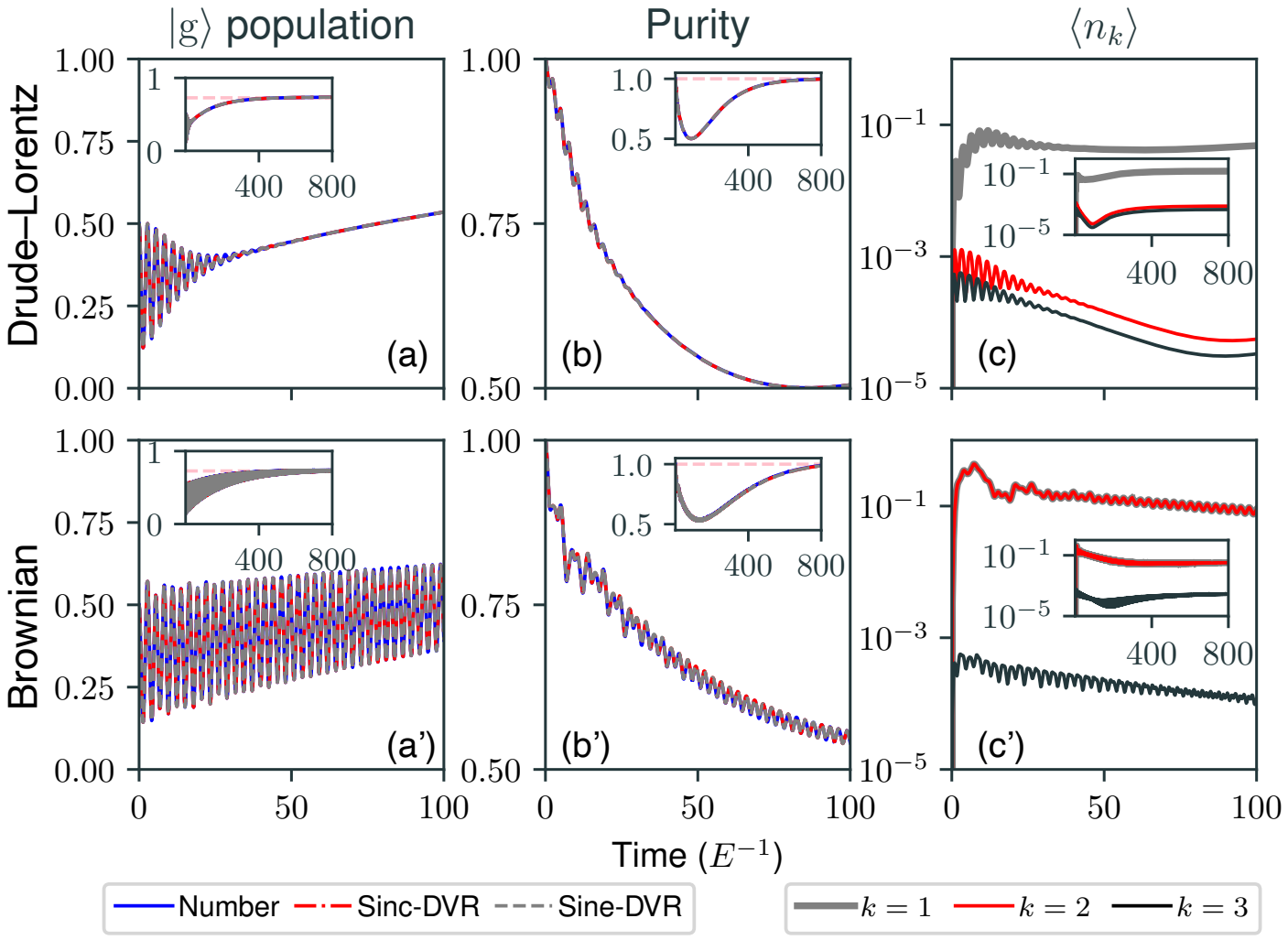

The curse of dimensionality in HEOM

Memory needs grow exponentially with number of features

$$\mathcal{O}(N^K)$$

Model spectral density

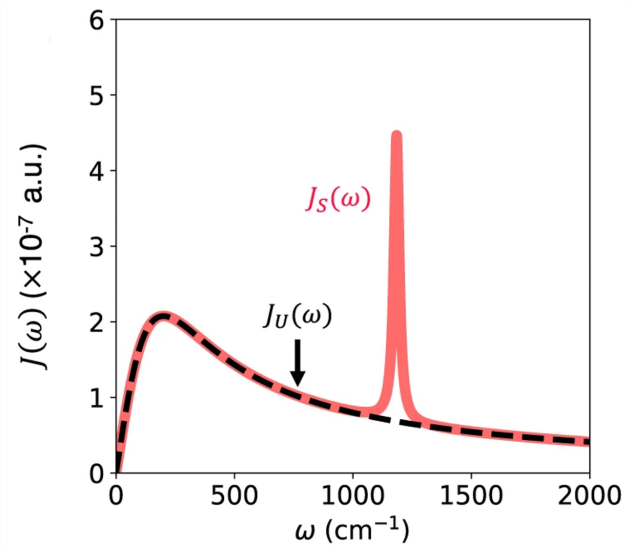

L. P. Lindoy, et al., *Nat. Commun.* 14, 2733 (2023)

K: typically $1 \sim 5$.

Realistic spectral density

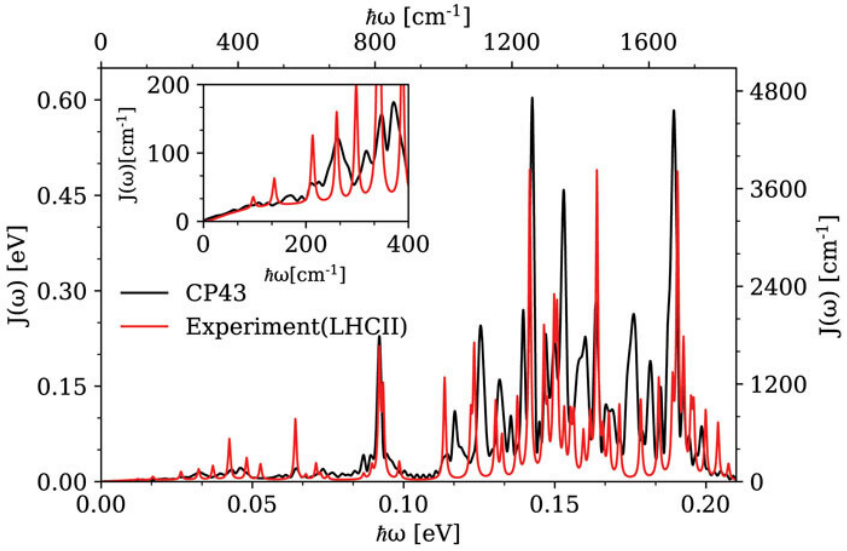

K: 10s to 100s.

Approaches to curb the curse of dimensionality

More efficient BCF decomposition schemes, e.g.

Dé, Jaouadi, Mangaud, Chin and Desouter-Lecomte,
JCP **160**, 244102 (2024)

Filter out near-zero ADMs

Q. Shi, L. Chen, G. Nan, R.-X. Xu, and Y. Yan,
JCP **130**, 084105 (2009)

Tree Tensor Network HEOM and TENSO

Chen and Franco *J. Chem. Phys.* **163**, 104109 (2025)

Editor's Pick!
Cover Article!

https://github.com/ifgroup/pytenso

- Enables HEOM computations with highly structured environments
- Implements tensor trains and tensor trees
- Three propagation strategies (Direct, PS1 and PS2)
- Fixed and variable rank propagation strategies
- Allows for time-dependent driving and non-commuting fluctuations
- Open-source code TENSO

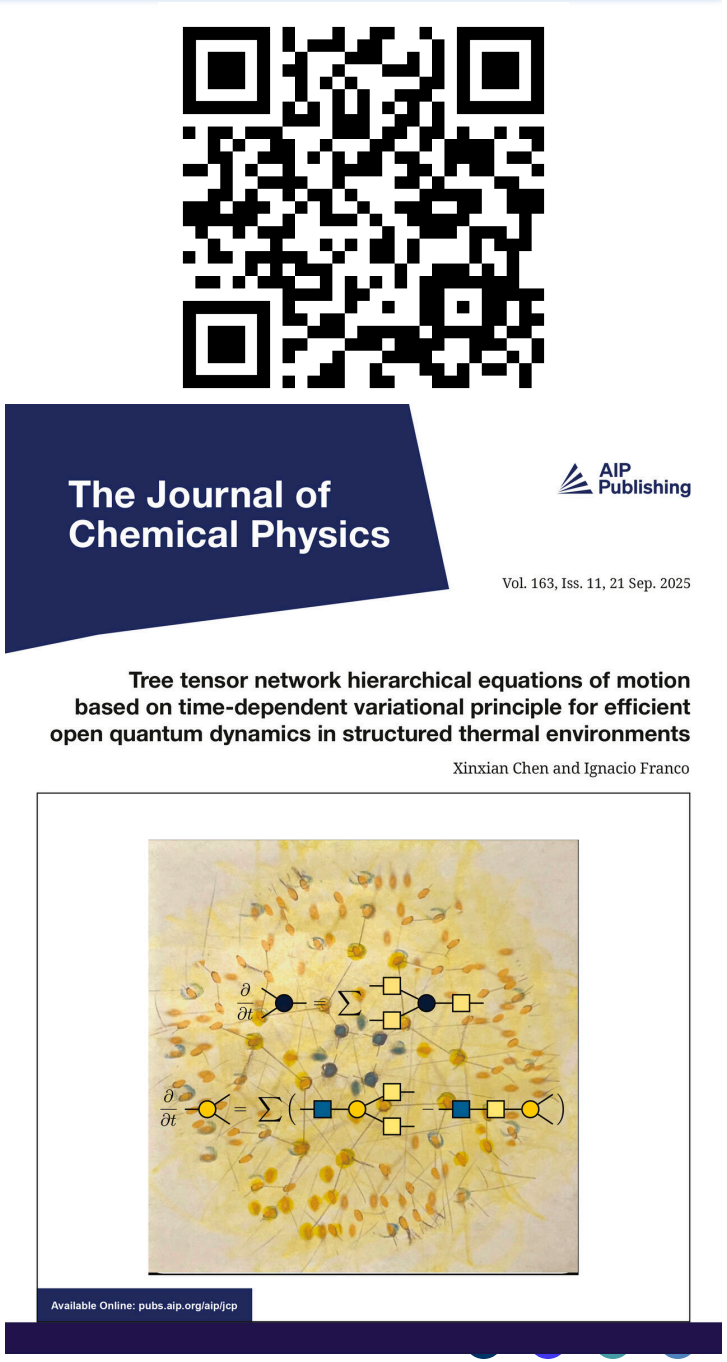

Other HEOM Tensor Network Efforts

Tensor Train — Y. Yan, M. Xu, T. Li, and Q. Shi, JCP **154**, 194104 (2021)

Tensor Tree — Y. Ke, R. Borrelli, and M. Thoss, JCP **156**, 194102 (2022)

Y. Ke JCP **158**, 211102 (2023)

Fixed Rank + Propagator based on Trotter Splitting
No need for master equations for core tensors

Our Work — Chen and Franco JCP **163**, 104109 (2025)

Tensor Trees + Trains

Master equation for core tensors

Arbitrary Tree Geometry

Arbitrary Order for Tensors

Fixed and Variable Rank

Three Propagation Strategies

Singular Value Decomposition (SVD)

$$A_{ij} = \sum_{k=1}^{R} U_{ik} s_k V_{jk}^*$$

$$U^\dagger U = V^\dagger V = \hat{1}$$

semi-unitary matrices

s_k : singular values $(s_1 \geq s_2 \geq s_K \geq 0)$

Keep the R largest singular values to compress redundant information in an array

Raw $(R = 587)$ $R = 5$ $R = 10$ $R = 20$ $R = 50$

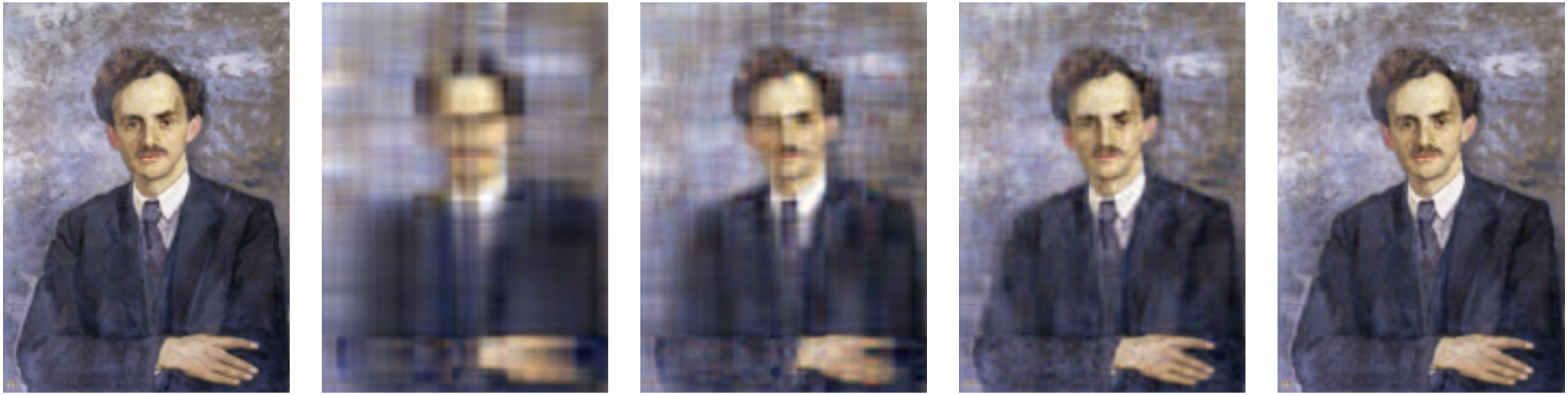

From SVD to Tree Tensor Network (TTN)

TTN: repeated SVDs of a high-order tensor

Tensor Train

$$A_{n_1\cdots n_6} = \sum_{a_1 a_2 a_3} C_{n_1 n_2 a_1} U^{(1)}_{a_2 n_3 a_1} U^{(2)}_{a_3 n_4 a_2} U^{(3)}_{n_5 n_6 a_3}.$$

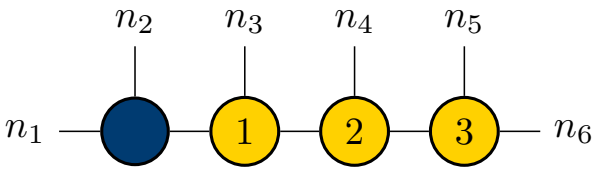

Tensor Tree

$$A_{n_1\cdots n_6} = \sum_{a_1 a_2 a_3} C_{n_1 n_2 a_1} U^{(1)}_{a_2 a_3 a_1} U^{(2)}_{n_3 n_4 a_2} U^{(3)}_{n_5 n_6 a_3}$$

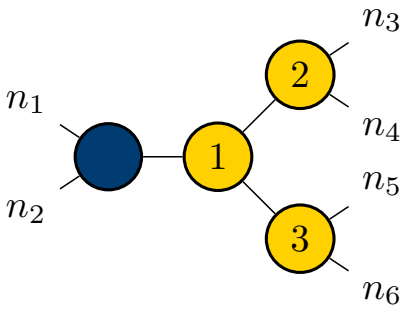

Root Tensor

Semi-Unitary Tensors

$$\sum_{\alpha\beta} U^{\star}_{\alpha\beta\gamma} U_{\alpha\beta\gamma'} = \delta_{\gamma\gamma'}$$

TTN decomposition of the extended density operator

Hypothesis: There is significant redundancy in the bexcitonic space that can be compressed

Extended Density Operator

$$|\Omega(t)\rangle \equiv \sum_{\vec{n}} \varrho_{\vec{n}}(t)|\vec{n}\rangle$$

Put all ADMs in a high-order tensor

$$\Omega_{ijn_1\ldots n_K} = (\rho_{\vec{n}})_{ij}$$

Tree-Tensor Network Decomposition

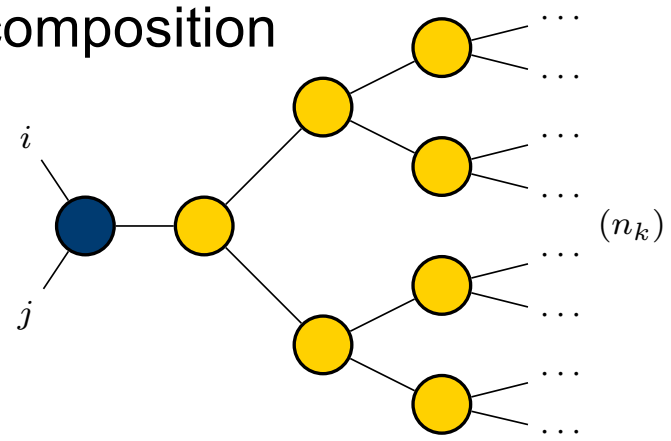

Bexciton indexes in the leaves

System indexes in the root tensor

Polynomial space complexity with *K* (!)

$$\mathcal{O}((M^2+N^2)R + KR^2N)$$

Sum of product form for the generator of the dynamics

$$\frac{\mathrm{d}}{\mathrm{d}t}\Omega(t) = \mathcal{L}(t)\Omega(t)$$

$$\mathcal{L}(t) = -\mathrm{i}H_{\mathrm{S}}^{\times}(t) + \sum_{k=1}^{K}\mathcal{D}_k = \sum_{m} h_m^{>}(t) \otimes h_m^{<}(t) \otimes h_m^{(1)} \otimes \cdots \otimes h_m^{(K)}.$$

m	$h_m^{>}(t)$	$h_m^{<}(t)$	$h_m^{(k)}$
1	$-\mathrm{i}H_{\mathrm{S}}(t)$	$\hat{1}$	$\hat{1}$
2	$\hat{1}$	$\mathrm{i}H_{\mathrm{S}}(t)$	$\hat{1}$
$5k-2$	$\hat{1}$	$\hat{1}$	$\gamma_{kk}\hat{n}_k$
$5k-1$	$c_k Q_{\mathrm{S}}$	$\hat{1}$	$\hat{z}_k^{-1}\hat{\alpha}_k^{\dagger}$
$5k$	$\hat{1}$	$-\bar{c}_k Q_{\mathrm{S}}$	$\hat{z}_k^{-1}\hat{\alpha}_k^{\dagger}$
$5k+1$	$-Q_{\mathrm{S}}$	$\hat{1}$	$\hat{\alpha}_k\hat{z}_k$
$5k+2$	$\hat{1}$	Q_{S}	$\hat{\alpha}_k\hat{z}_k$

Parallel to Multi-configurational time-dependent Hartree

H. Wang and M. Thoss, JCP **119**, 1289 (2003)

Master Equation for Core Tensors

Time Dependent Variational Principle

$$\sum_{ijn_1\cdots n_K} [\delta\Omega(t)]^{\star}_{ijn_1\cdots n_K} \left[\left(\mathcal{L} - \frac{\mathrm{d}}{\mathrm{d}t}\right)\Omega(t)\right]_{ijn_1\cdots n_K} = 0$$

Root Tensor – Simpler Dynamics

$$\left[\frac{\partial}{\partial t}\right.$$


$$= \sum_m$$
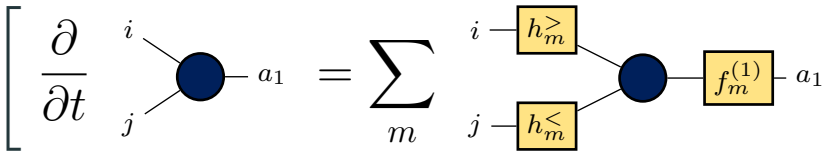

$$\left.\right]$$

$$\frac{\partial}{\partial t} A^{(0)}_{i'j'a_1'} = \sum_m \sum_{ija_1} [h_m^{>}]_{i'i} [h_m^{<}]_{j'j} [f_m^{(1)}]_{a_1'a_1} A^{(0)}_{ija_1}$$

Non-Root Tensors – Requires Regularization

$$\frac{\partial}{\partial t} U^{(s)}_{a_s''\beta'\gamma'} = \sum_m \sum_{a_s'a_s\beta\gamma} [\mathcal{C}_m^{(s)}]_{a_s'a_s''} \left([f_m^{(\beta)}]_{\beta'\beta} [f_m^{(\gamma)}]_{\gamma'\gamma} U^{(s)}_{a_s'\beta\gamma} - U^{(s)}_{a_s\beta'\gamma'} [f_m^{(s)}]_{a_sa_s'} \right)$$

$$\left[\frac{\partial}{\partial t}\right.$$
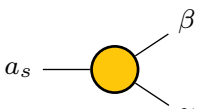

$$= \sum_m \Bigg($$
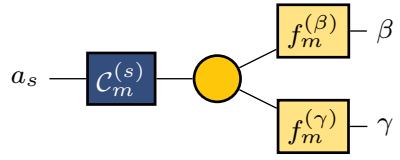

$$-$$
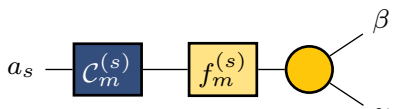

$$\Bigg)\left.\right]$$

Propagation Strategies

Adapt propagation strategies from MCTDH to the TTN-HEOM

Projector Splitting 1

- Trotterization algorithm. Errors determined by split time step
- Challenging to parallelize
- Fixed rank
- Used by Ke in JCP 158, 211102 (2023)

Projector Splitting 2

- Similar features to PS1
- Two-site algorithm
- Adaptive rank

Direct Propagation of Master Equation for Core Tensors

- Admits high-order numerical propagation schemes (e.g. Runge-Kutta) and their parallelization
- Requires regularization like in MCTDH (specially at early times)
- Fixed rank

THIS WORK

TENSO

- Implemented in Python with NumPy and PyTorch
- Supports HEOM/ML-MCDTH/etc in a unified framework
- Supports direct integration, PS1, PS2 and mixed strategies for propagation
- Can handle structured baths for molecular systems
- Arbitrary tensor trees and tensor order
- Open source and available on GitHub

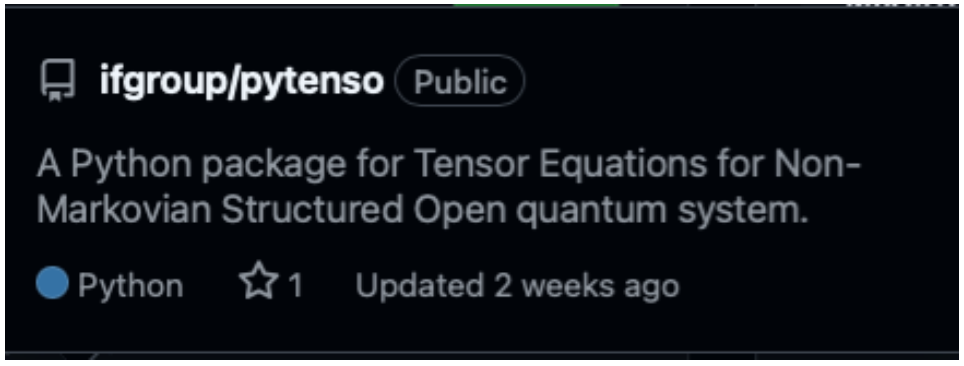

https://github.com/ifgroup/pytenso

TTN-HEOM vs HEOM: Drude-Lorentz Bath

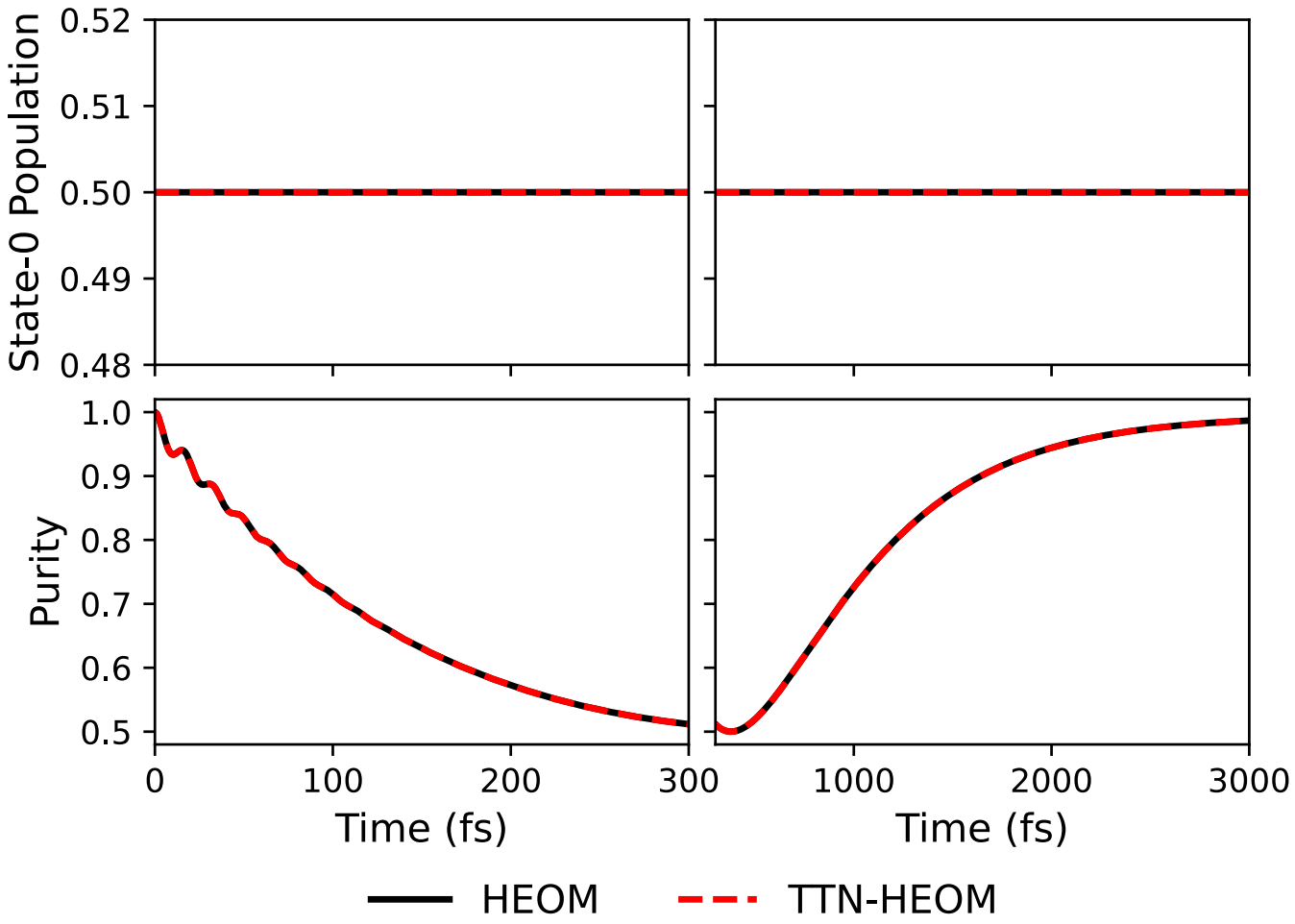

Figure 4.3 Comparison between the HEOM and the TTN-HEOM for a two-level system $\{|0\rangle, |1\rangle\}$ interacting with a Drude-Lorentz bath. The plots show the population and purity dynamics for the system $H_{\mathrm{S}} = V\sigma_x$ with $V = 1000\ \mathrm{cm}^{-1}$ coupled to a Drude-Lorentz bath with $\lambda_0 = 200\ \mathrm{cm}^{-1}$ and $\gamma_0 = 100\ \mathrm{cm}^{-1}$. The system operator Q_{S} is chosen as $\sigma_z/2$ such that $[H_{\mathrm{S}}, H_{\mathrm{SB}}] \neq 0$. The initial system is a pure one as $|\psi_{\mathrm{S}}(t=0)\rangle = (|0\rangle + |1\rangle)/2$. As to the HEOM parameters, $N_k = 10$ is chosen for each bexciton to guarantee the convergence in depth, and the direct integration with a rank of 10 is used for TTN-HEOM.

Example: Two-surface molecule

$$H_S = \frac{E}{2}\sigma_z + V\sigma_x \qquad Q_S = \sigma_z \qquad |\psi\rangle = \frac{1}{\sqrt{2}}(|0\rangle + |1\rangle)$$

Spectral density for thymine in 300 K water

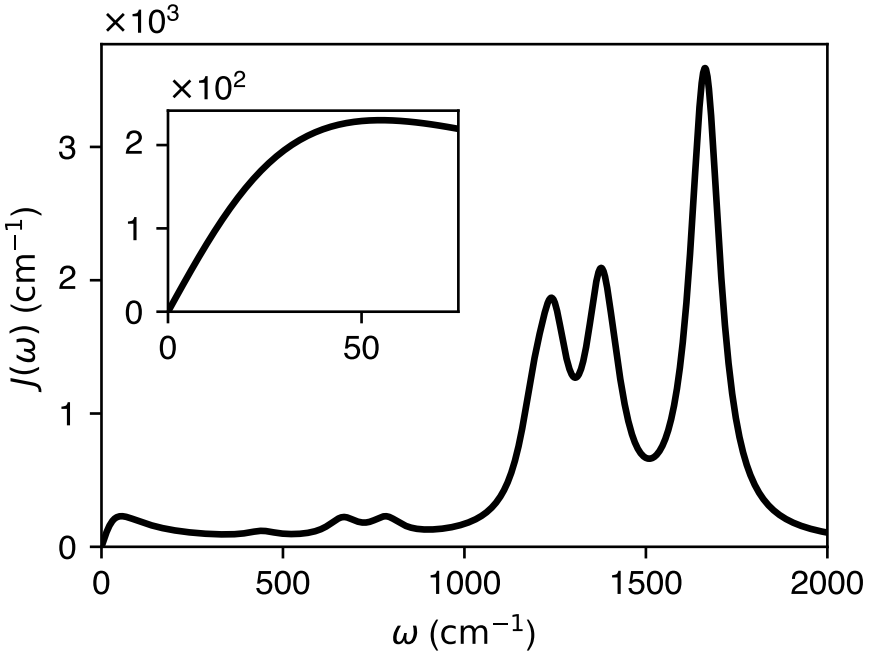

Bath Features $K = 20$

1 from Drude-Lorentz solvent
16 from Brownian Oscillators
3 from low temperature corrections (Padé)

Impossible for other HEOM implementations

Gustin, McCamant, Franco PNAS **120**, e2309987120 (2023)

	Balanced Tree			Train			Dense HEOM
Rank	40	60	80	40	60	80	—
Size ($\times 10^6$)	0.7	2.2	4.9	0.6	1.3	2.3	4.2×10^{20}

Table 4.2 The size (overall number of core tensor elements) of TTN for a bath described by 20 features and a depth of 20 for each N_k. The memory usage of a dense high-order EDO tensor in HEOM is also showed for comparison.

Consistency between propagation strategies

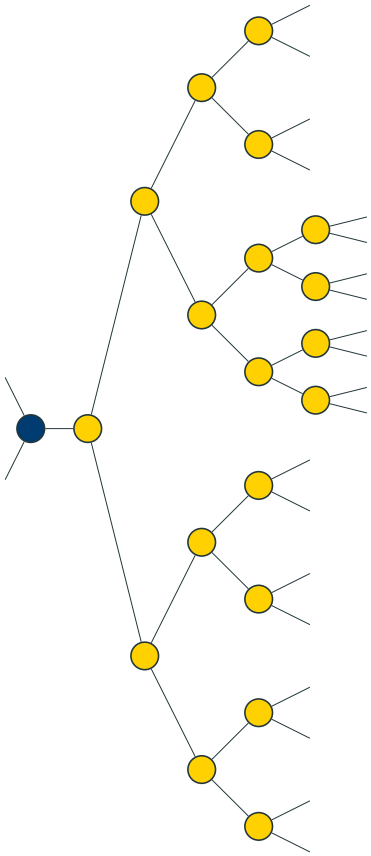

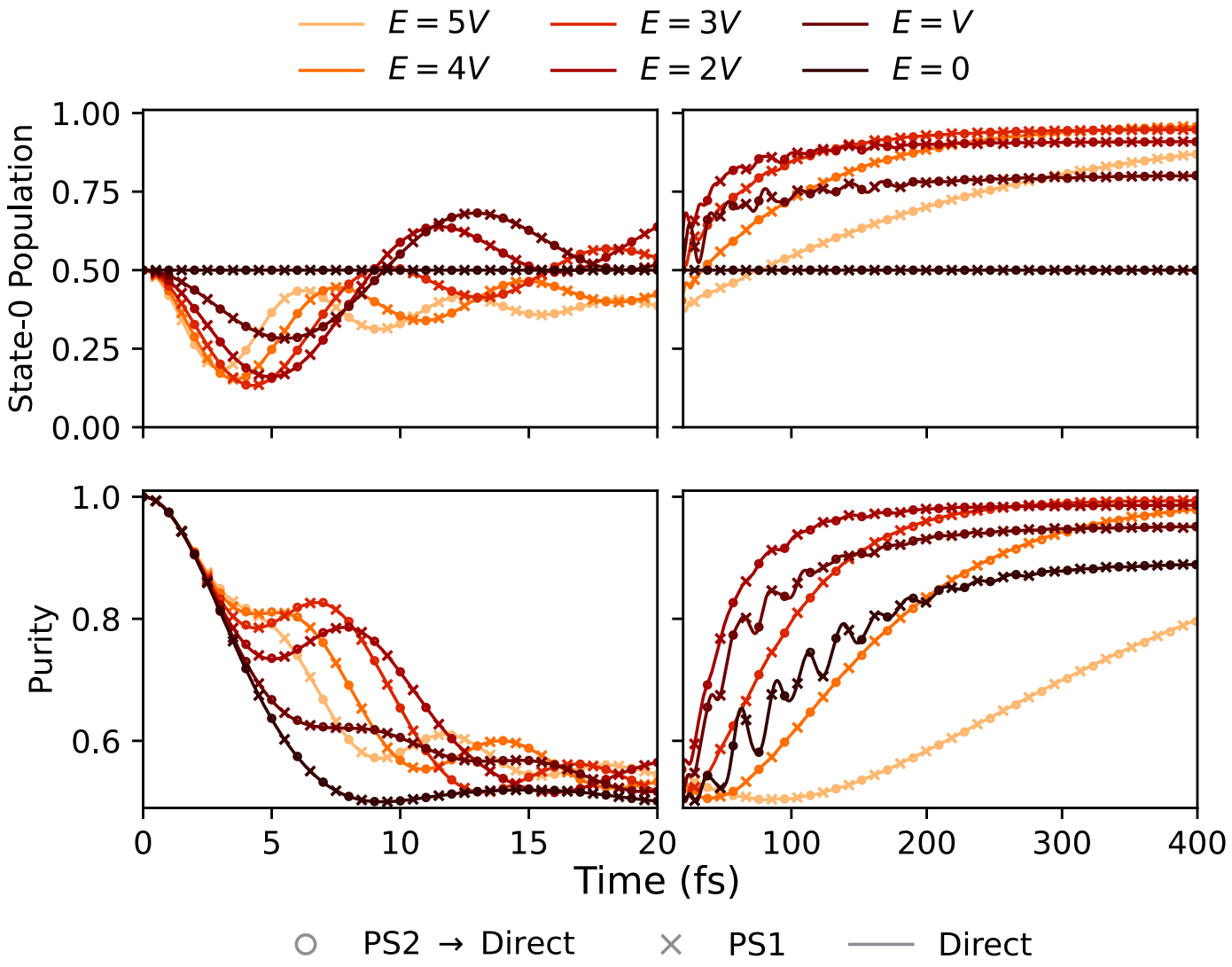

Performance differences

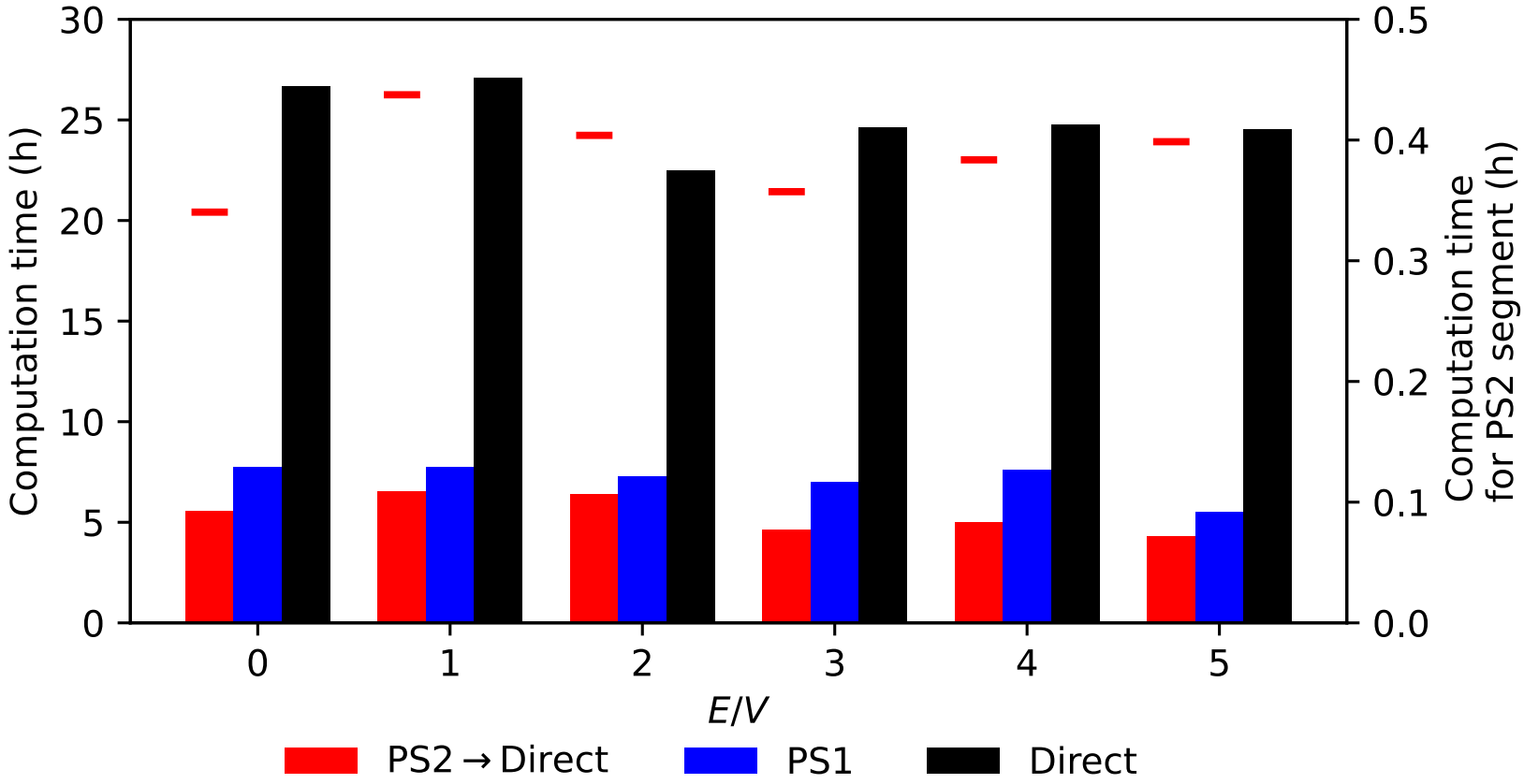

Mixed strategy (PS2 to Direct) is the fastest

PS2 determines the ranks from initial-time dynamics
Direct propagation is efficient (after very early times)

Trees vs. Trains

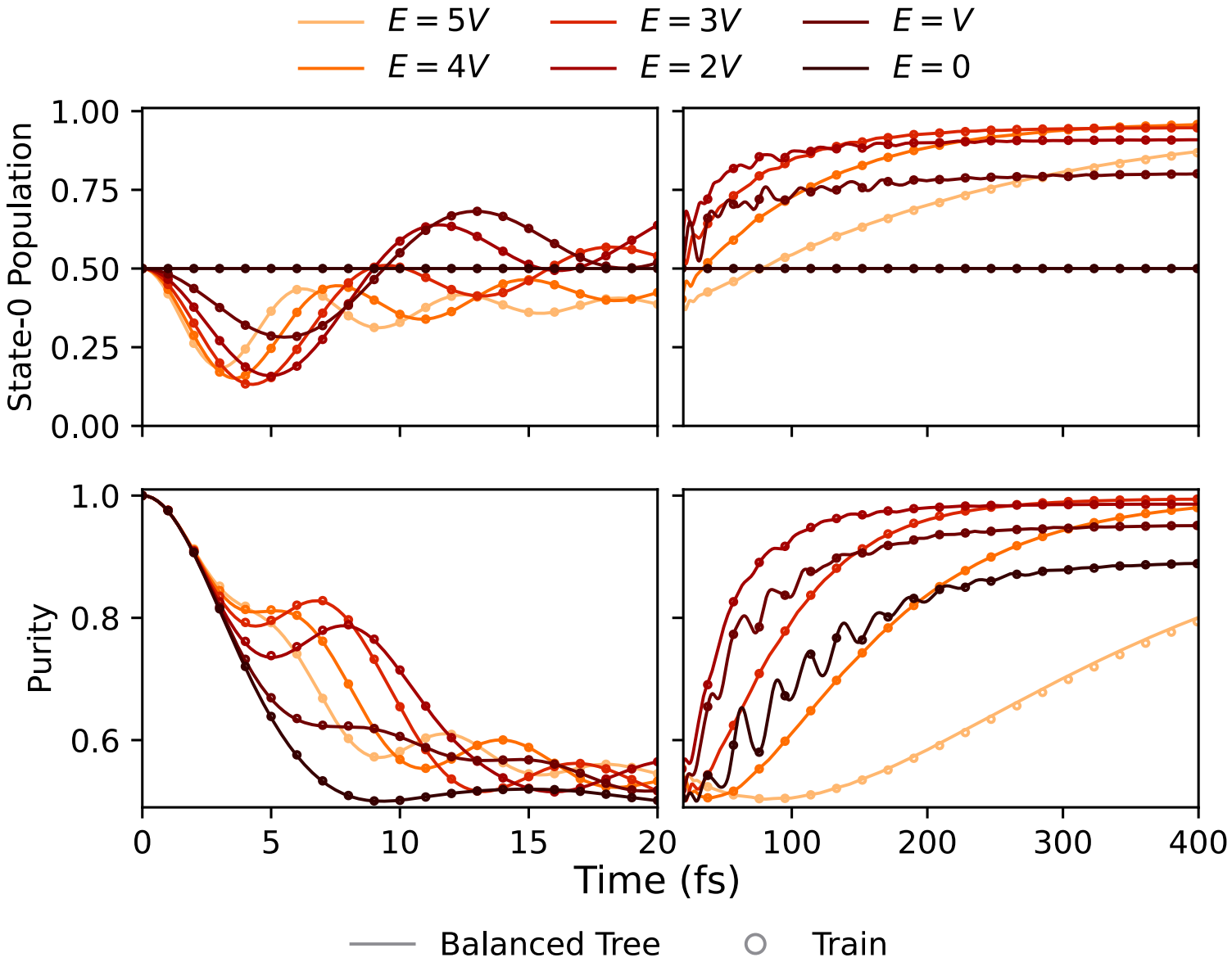

PS2 to Direct

3-site Fenna-Matthews-Olson Complex

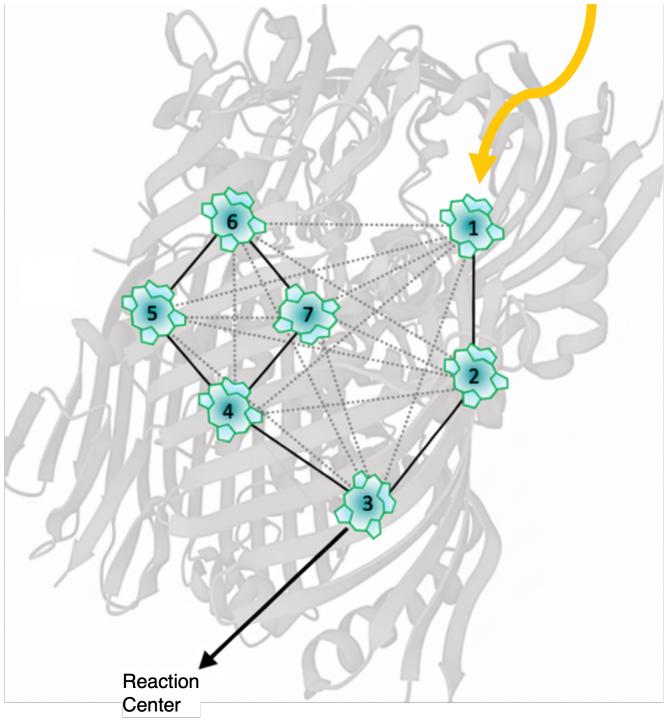

Phys. Rev. Appl. 23, 044061 (2025)

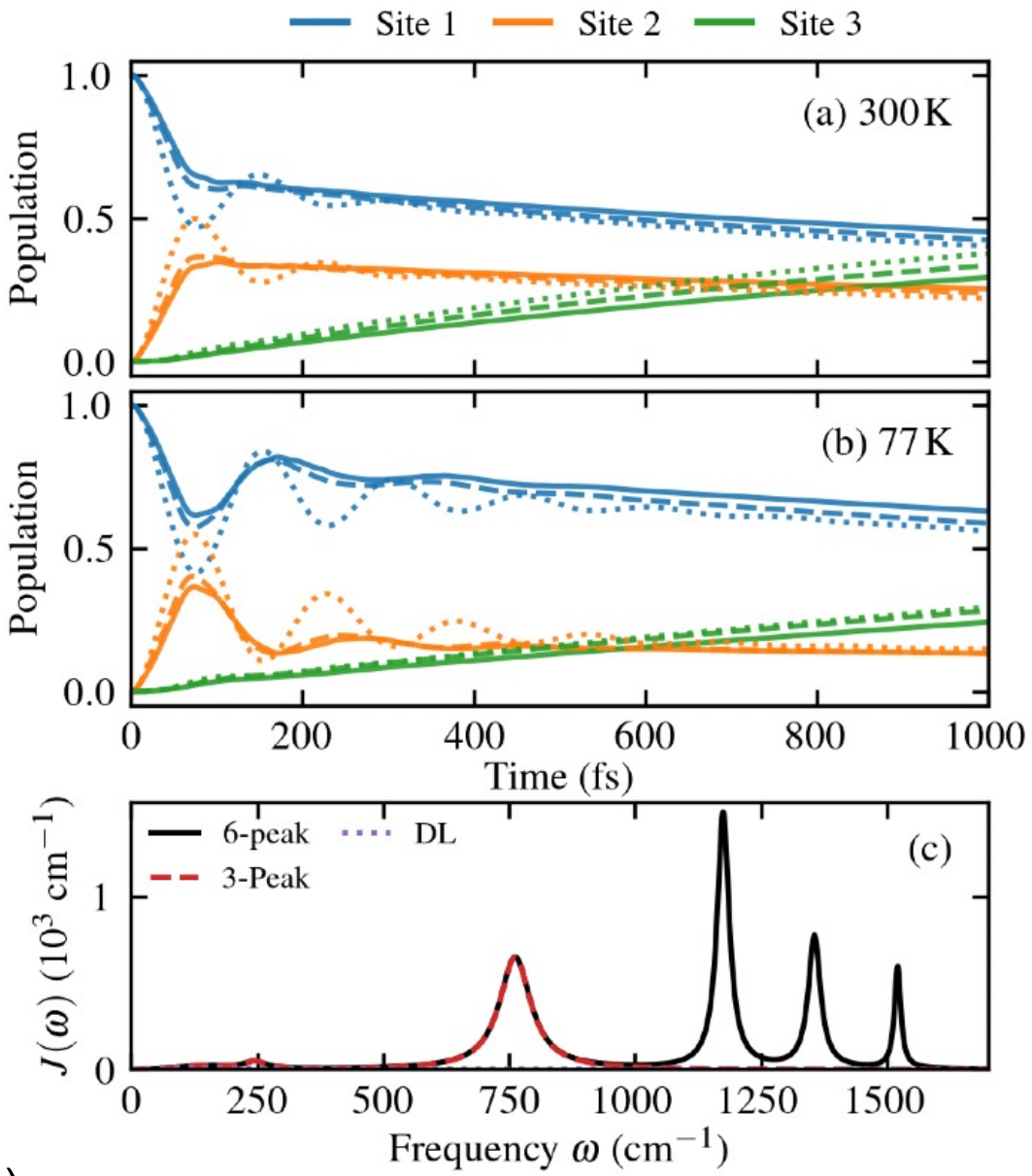

Ishizaki et al. PNAS 106, 17255 (2009)

Tree Tensor Network HEOM and TENSO

Xinxian Chen and IF, J. Chem. Phys. **160**, 204116 (2024)
J. Chem. Phys. **163**, 104109 (2025)

https://github.com/ifgroup/pytenso

- Enables HEOM computations with highly structured environments
- Implements tensor trains and tensor trees
- Three propagation strategies (Direct, PS1 and PS2)
- Fixed and variable rank
- Arbitrary tensor order
- Allows for time-dependent driving and non-commuting fluctuations
- Open-source code TENSO

Usage Paper: Available Soon!

TENSO: Software Package for Numerically Exact Open Quantum Dynamics Based on Efficient Tree Tensor Network Decomposition of the Hierarchical Equations of Motion

Juan C. Rodriguez,[1] Michelle Anderson,[1] Luchang Niu,[2] Xinxian Chen,[1] and Ignacio Franco[1, 2, 3, a)]
[1)] *Department of Chemistry, University of Rochester, Rochester, New York 14627, United States*
[2)] *Department of Physics and Astronomy, University of Rochester, Rochester, New York 14627, United States*
[3)] *The Institute of Optics, University of Rochester, Rochester, New York 14627, United States*

(Dated: 11 February 2026)

TENSO is a versatile and powerful open-source software package for numerically exact simulations of the dynamics of quantum systems immersed in structured thermal environments. It is based on a tree tensor network decomposition of the hierarchical equations of motion (HEOM) that efficiently curbs its curse of dimensionality with bath complexity. As such, TENSO enables exact non-Markovian open quantum dynamics simulations even with complex environments typical of chemistry and quantum information science. TENSO allows for time-dependent drive in the system, and for non-commuting fluctuations. More generally, TENSO efficiently propagates the dynamics for any method with a generator of the dynamics that can be expressed in a sum-of-products form, including the HEOM and multi-layer multiconfigurational time-dependent Hartree methods. TENSO enables simulations using tensor trees and trains of arbitrary order, and implements three propagation strategies for the coupled master equations; two fixed-rank methods that require a constant memory footprint during the dynamics and one adaptive rank method with a variable memory footprint controlled by the target level of computational error. In contrast to the accompanying theory and algorithmic paper [J. Chem. Phys. **163**, 104109 (2025)] the focus here is on the practical usage and applications of TENSO with underlying theoretical concepts introduced only as needed.

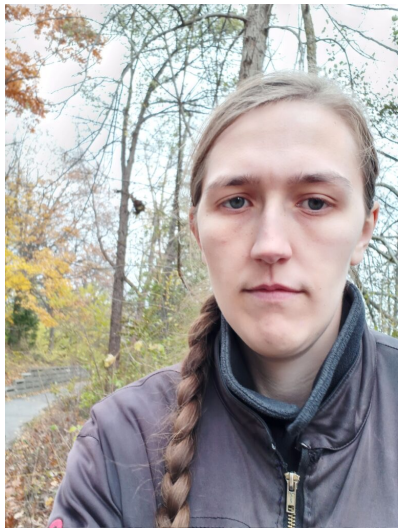

Thanks!

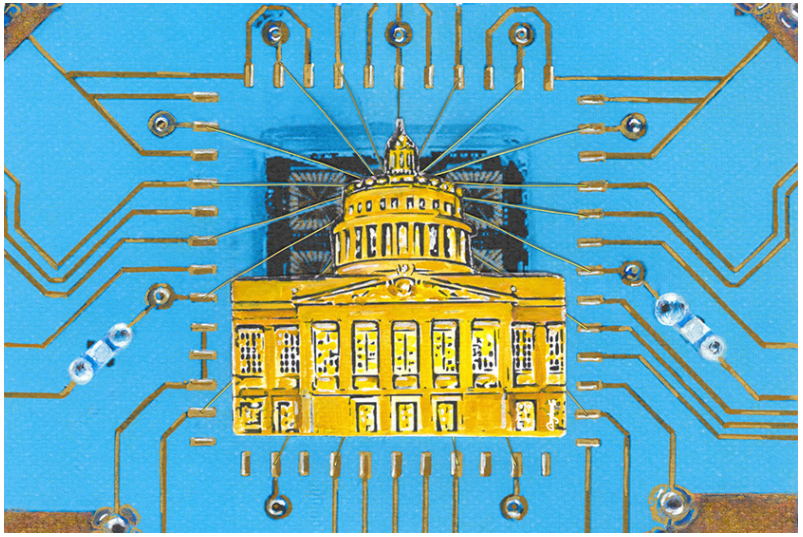

UR Center for Coherence and Quantum Science

DOE DE-SC0025334
NSF CHE-2416048
NSF CHE-2511834
NSF PHYS-2310657

Chemical Principles of Quantum Decoherence

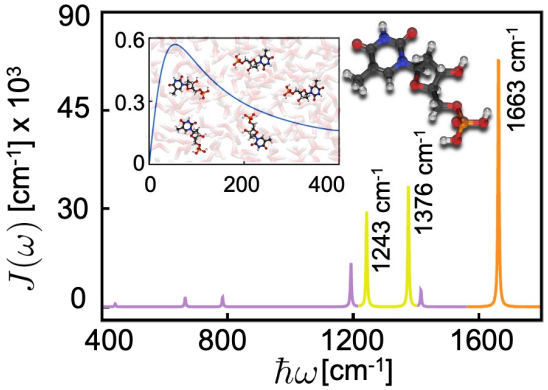

PNAS **120**, e2309987120 (2023)

Foundations of Decoherence

e.g. JCP **162**, 064106 (2025);
JPCL 13, 11503 (2022);
JCP **151**, 014109 (2019);
JCP, **148**, 134304 (2018);
JPCL **9**, 773 (2018)

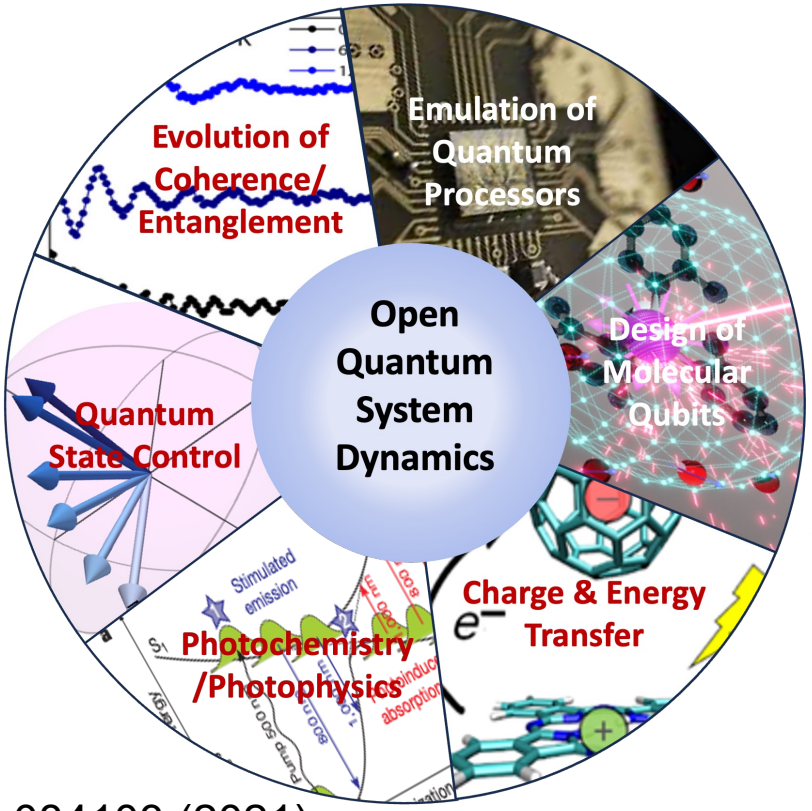

Quantum Simulation

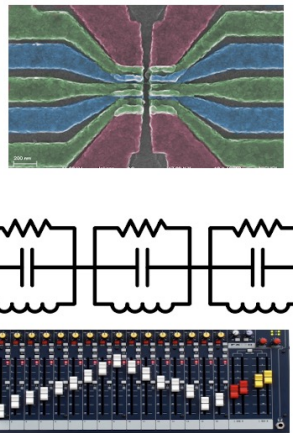

PRX Quantum **3**, 040308 (2022); JPC A **129**, 15, 3587 (2025)

Theory of Dissipation Pathways

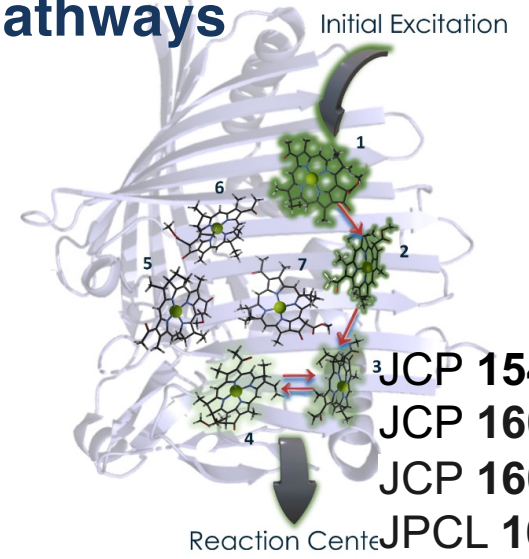

JCP **154**, 084103 (2021);
JCP **160**, 214111 (2024);
JCP **160**, 214112 (2024);
JPCL **16**, 13093 (2025);
JCP **164**, 034105 (2026)

Tensor Network Strategies

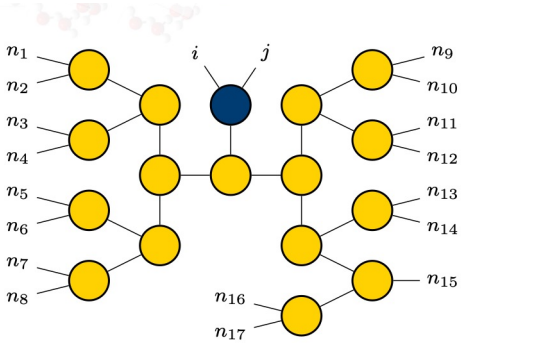

JCP **160**, 204116 (2024);
JCP **163**, 104109 (2025);
JCP **164**, 024112 (2026)